HAL
open science

Assessing the durability of nuclear glass with respect to silica controlling processes in a clayey underground disposal

Stéphanie Leclerc, Laurent de Windt, Stéphanie Leclercq, Jan van Der Lee

To cite this version:

Stéphanie Leclerc, Laurent de Windt, Stéphanie Leclercq, Jan van Der Lee. Assessing the durability of nuclear glass with respect to silica controlling processes in a clayey underground disposal. Scientific Basis for Nuclear Waste Management, 2006, Ghent, Belgium. pp.313-320. hal-00596569

HAL Id: hal-00596569

https://minesparis-psl.hal.science/hal-00596569

Submitted on 15 Feb 2021

HAL is a multi-disciplinary open access archive for the deposit and dissemination of scientific research documents, whether they are published or not. The documents may come from teaching and research institutions in France or abroad, or from public or private research centers.

L'archive ouverte pluridisciplinaire **HAL**, est destinée au dépôt et à la diffusion de documents scientifiques de niveau recherche, publiés ou non, émanant des établissements d'enseignement et de recherche français ou étrangers, des laboratoires publics ou privés.

Assessing the durability of nuclear glass with respect to silica controlling processes in a clayey underground disposal

Laurent De Windt[1], Stéphanie Leclercq[2] and Jan van der Lee[1]

[1] Ecole des Mines de Paris, CIG, 77300 Fontainebleau, France

[2] Electricité de France, R&D, 77818 Moret sur Loing, France

ABSTRACT

The long-term behaviour of vitrified high-level waste in an underground clay repository was assessed by using the reactive transport model HYTEC with respect to silica diffusion, sorption and precipitation processes. Special attention was given to the chemical interactions between glass, corroded steel and the host-rock considering realistic time scale and repository design. A kinetic and congruent dissolution law of R7T7 nuclear glass was used assuming a first-order dissolution rate, which is chemistry dependent, as well as a long-term residual rate. Without silica sorption and precipitation, glass dissolution is diffusion-driven and the fraction of altered glass after 100,000 years ranges from 5% to 50% depending on the fracturation degree of the glass block. Corrosion products may limit glass dissolution by controlling silica diffusion, whereas silica sorption on such products has almost no effect on glass durability. Within the clayey host-rock, precipitation of silicate minerals such as chalcedony may affect glass durability much more significantly than sorption. In that case, however, a concomitant porosity drop is predicted that could progressively reduce silica diffusion and subsequent glass alteration.

INTRODUCTION

The alteration or dissolution rate of borosilicate glasses depends on the dissolved silica concentration in the bulk solution. As the aqueous concentration rises, the rate decreases down to a long-term value that is many orders of magnitude lower that the initial rate. In addition to a control by chemical affinity, this significant decrease results from the formation of a dense protective gel acting as a diffusive barrier at the glass/solution interface [1]. Whatever the underlying processes, several lab experiments have proved that glass dissolution is clearly enhanced by the presence of clay minerals, and to a lesser extent, of steel corrosion products [2-4]. Silica diffusion followed by sorption and/or precipitation are potential underlying mechanisms, albeit their long-term relevance is still a debated question.

Previous studies have addressed the lifetime of nuclear glass under clayey disposal conditions according to analytical models [5,6]. In the present study, the durability of vitrified high-level waste (HLW) is assessed by using a reactive transport code – i.e., a numerical code coupling chemistry and hydrodynamics – with respect to silica diffusion, sorption and precipitation processes. Numerical modelling provides not only means to extrapolate glass dissolution data to long periods of time and to representative repository designs in terms of geometry and material masses, but also to consider detailed chemical processes at a mechanistic level for a full set of interacting chemical elements. A special attention is given to the chemical interactions between glass, corroded steel and the clayey host-rock in the near-field.

DISPOSAL AND MODELLING FEATURES

Disposal concept and materials

The host-rock formation properties are those of stiff clays such as can be found in France: an indurated claystone with low water content and diffusion as the predominant transport process. A common effective diffusive coefficient, $D_{eff\text{-}HR}$, of $2x10^{-11}$ m^2/s was considered for all the dissolved species. The mineralogy is characterized by a high content in clay minerals, quartz, calcite, dolomite and pyrite for a cation exchange capacity (CEC) of 20 meq/100g of rock.

The disposal concept consists of horizontal tunnels of small diameters consolidated by linings of steel but without backfill materials. The excavated damaged zones ($D_{eff\text{-}EDZ} = 1x10^{-10}$ m^2/s) are thus restricted to a dozen of centimetres only. The waste package consists of a nuclear glass zone with a diameter of 0.44 m (glass block + interstices), and a low alloyed steel canister, 0.055 m thick. The liner is also made of low alloyed steel and has a thickness of 0.025 m. An average temperature of 50°C was considered in the calculations.

The steel waste canister and the tunnel lining were both assumed to be corroded after 1,000 years allowing for water to saturate the medium and diffusive transfers to occur in the waste zone. Magnetite was introduced as the main corrosion product, but steel corrosion mechanisms were not explicitly taken into account in the modelling. Magnetite, which has a higher molar volume than metallic iron, was assumed to fill the interstice voids. It is not obvious to attribute an effective diffusion coefficient to this magnetite-enriched zone. A relatively high $D_{eff\text{-}mag}$ value of $1x10^{-10}$ m^2/s was considered in the present calculations, though a less conservative value of $1x10^{-11}$ m^2/s was also selected in test-case III for sensitivity analysis as explained below.

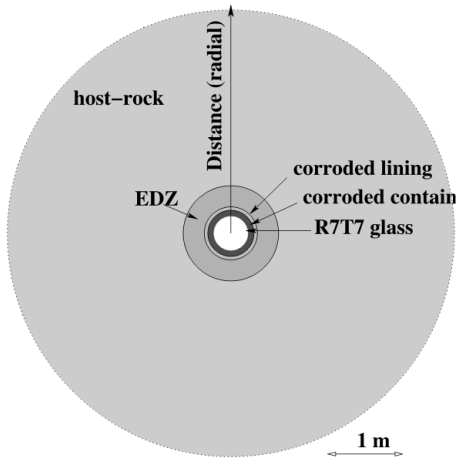

Figure 1. Simplified disposal configuration considered in the calculations (assuming radial symmetry).

Modelling approach and data

The calculations presented herein were carried out with the reactive transport code HYTEC[7] in radial symmetry, i.e. equivalently to a 2-D transversal cross-section of the disposal tunnel (see Figure 1). All simulations were based on the local equilibrium assumption, except for glass dissolution. The thermodynamic data were compiled from the EQ3/6-LLNL database. Silica sorption was simulated according to the double layer surface complexation theory. A data set has been obtained experimentally for magnetite [8,9], but derived from a distribution coefficient (Kd = 0.05 kg/m^3) for the host-rock [3,10]. The sorption data (ionic exchange and surface complexation) were taken from literature [11,12]. Sorption was only taken into account for Ca-H-K-Na-Si, and not for the other glass constituents, in a first approximation. Precipitation

of neoformed silicate phases was not allowed in the entire system, neither in the waste zone nor in the host-rock, except for test-case IV as explained in the results section.

A simplified R7T7 glass composition was considered including the glass network formers B-Si-O, the modifiers Na-Ca and two radioactive elements Cs-I. Glass alteration kinetics start with fast interdiffusion and network hydrolysis reactions to become controlled by the formation of a gel layer in a second step. These processes can be explicitly simulated in very small-scale models [13]. Lumping these small-case processes together in terms of a global parametric kinetic rate-law, however, has the advantage of being operational for models at the scale of a waste-disposal. Assuming congruent dissolution of the glass matrix, the kinetic process was described by the combination of a first-order dissolution rate R [3], dependent of the bulk solution chemistry (pH, orthosilisic acid activity),

$$R = k\,S\left(H^{+}\right)^{-0.4}\left(1-\frac{\left(H_4SiO_4\right)}{C^{*}}\right) \tag{1}$$

and a long-term residual dissolution rate, R_r, which is chemistry independent [14],

$$R_r = k_r\,S \tag{2}$$

The parenthesis stands for the species activity in the bulk solution, k and k_r are dissolution rate constants, C* is a saturation threshold for which the first-order dissolution stops, and the total surface S depends on the degree of fracturation of the vitrified waste. The dissolution rate terms are both temperature-dependent. Table I gives the parameter values used throughout this paper.

The approach followed here is similar, though simplified, compared to the LIXIVER-2 model [3]. Silica diffusion and sorption within the gel layer are not explicitly taken into account in our model and, consequently, there is no incongruent leaching of silica and boron/alkalis from the glass. Furthermore, an Elementary Representative Volume (ERV) approach was used for

spatial discretization. Water intrusion and glass dissolution were allowed within the whole glass zone, due to the cracking of the R7T7 block, and not at the glass/canister boundaries only. With this respect, the effective diffusion coefficient, $D_{eff\text{-}glass}$, assumed for silica and the other glass elements inside the (fractured) glass zone was $5x10^{-10}$ m^2/s. The common parameter S of Eqs (1) and (2) corresponds – conservatively - to the entire available surface, including the outer cylindrical surface and the internal fracture surfaces. It is worth mentioning that, for most of the calculations presented here, the silica saturation threshold was reached inside the glass fractured zone and the glass matrix dissolved in these inner zones according to the residual rate only.

Table I. Kinetic parameters related to R7T7 glass dissolution, Eqs 1 and 2.

T	50° C	
k	$1.50\ 10^{-5}$ $g/m^2/d$	e.g. $k(H^+)^{-0.4} = 10^{-2}$ $g/m^2/d$ at pH = 7
k_r	$5.00\ 10^{-5}$ $g/m^2/d$	
C^*	$2.50\ 10^{-3}$ mol/L	
Total surface S (per glass block)	10 m^2	Fracturation ratio(*) = 5
	110 m^2	Fracturation ratio = 60

(*) Fracturation ratio FR = total surface/surface of the unfractured glass block.

Table II. Altered fraction (%) of the vitrified waste with respect to silica controlling processes.

	2,000 years	10,000 years	100,000 years
Test-case I (diffusion driven only)			
fracturation rate = 5	0.2	1.1	7.0
fracturation rate = 60	0.5	5.0	50.2

Test-case II (Si sorption on corroded steel)			
fracturation rate = 5	0.2 - 0.45(*)	1.1 - 1.35(*)	7.0 - 7.25(*)
fracturation rate = 60	0.5 - 0.75(*)	5.0 - 5.25(*)	50.2 - 50.45(*)
Test-case III (Si sorption on corroded steel and clayey host-rock)			
fracturation rate = 5	1.0	3.5	19.5
fracturation rate = 60	1.0	5.5	50.7
Test-case IV (Si precipitation in the clayey host-rock)			
fracturation rate = 60,			
$D_{eff\text{-}magnetite} = 1x10^{-10}$ m^2/s	1.9	65.0(**)	-
$D_{eff\text{-}magnetite} = 1x10^{-11}$ m^2/s	0.5	3.1	-

(*) Without considering pre-equilibrium of magnetite sorption site with host-rock dissolved silica.

(**) In the penalizing assumption of no feedback of mineral precipitation on diffusive transfers.

RESULTS AND DISCUSSION

Diffusion-driven base test-case

Four test-cases are considered introducing step by step the complexity of the chemical near-field interactions. Test-case I focuses on silica diffusion through the corroded steel components and within the host-rock without silica sorption and precipitation. For a minor fracturation ratio, the global proportion of altered glass remains low (~ 7% after 100,000 years, see Table II) in

agreement with glass lifetimes published in previous analytical studies [5,6]. Alteration is driven by silica diffusion, i.e. relatively fast at the beginning then followed by a gradual decrease. The diffusion process is mainly active at the outer parts of the vitrified waste zone open to the near-field environment (see Figure 2). The dissolved silica activity in solution remains slightly below the saturation term C^* in such zones corresponding to a very weak first-order dissolution rate. In contrast, saturation is reached in the inner volumes of the fractured glass, i.e. $(H_4SiO_4) \geq C^*$, preventing any R-type dissolution. The residual rate Rr which is independent on aqueous silica activities is nevertheless active in such inner zones. Calculations indicate a more pronounced effect when the fracturation state raises from 5 to 60, with a total altered fraction close to 50% in 100,000 years. Alteration remains, however, moderate over the first 10,000 years as reported in Table II, a time period corresponding to the highest radionuclide activity. A higher total surface S speeds up glass dissolution leading to a rapid saturation with respect to C^* and, consequently, to a residual dissolution and flat decrease in R7T7 content in the entire glass zone (Figure 2).

The R7T7 glass behaves like an alkaline mineral, leading to an increase of pH in the bulk solution with dissolution. Figure 2, however, shows almost no modification of the near-field pH for test-case I whatever the fracturation ratio. This is due to a dilution effect as well as buffering capacities of the host-rock through proton exchange with surface sites of the clay-minerals.

Fracturation ratio = 5 **Fracturation ratio = 60**

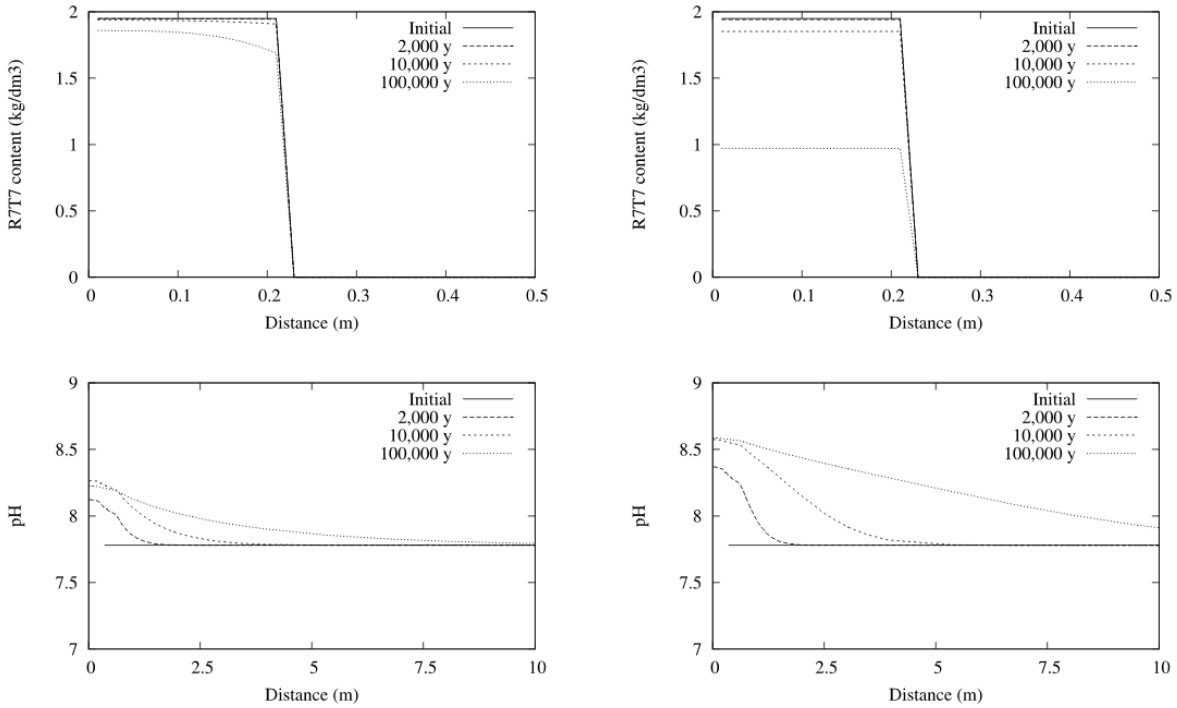

Figure 2. Evolution with time of R7T7 content (top) and pH profiles (bottom) for the diffusion-driven base case (test-case I) as a function of the fracturation ratio of the glass block.

Effects of steel corrosion products

The corroded container and liner, located at the vicinity of the vitrified waste, are the first materials that can control dissolved silica and glass alteration. Silica sorption on magnetite was therefore introduced in test-case II. At disposal time scales, sorption on magnetite has almost no effect on glass dissolution. The surface sites of silica are saturated by glass dissolution in one hundred years after canister failure. In comparison with test-case I, the total altered fraction is incremented by 0.25% only (Table II). Furthermore, the corrosion of the steel materials will most probably progress from the host-rock side. Hence, silica and others elements will migrate from

the host-rock and saturate the magnetite sorption sites before glass dissolution. For this reason, the results are found almost identical to those of the first test-case, if considering pre-saturation of the magnetite sorption sites. The role of magnetite on glass alteration enhancement could be neglected provided that precipitation of iron silicate minerals, in addition to sorption processes, does not take place. Silica precipitation may indeed amplify glass dissolution. Another point, positive this time, is that long-term expansion of corrosion product and subsequent porosity drop may generate a more efficient barrier against silica diffusion than assumed in the present calculations. This point is examined in the next section.

Silica controlling processes by the clayey host-rock

The third and fourth test-cases aim at investigating the possibility of a host-rock behaving like a silica sink by sorption and precipitation of new phases respectively, thus increasing the glass dissolution rate. Figure 3 clearly indicates that the profile of silica sorbed on host-rock

Fracturation ratio = 5

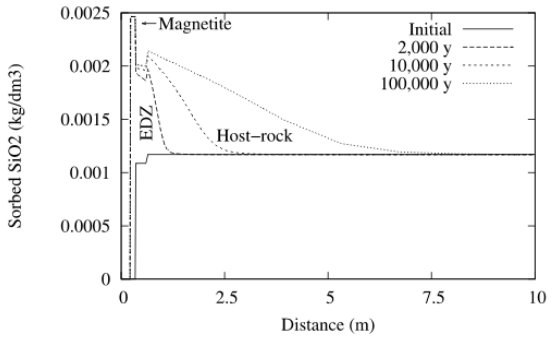

Fracturation ratio = 60

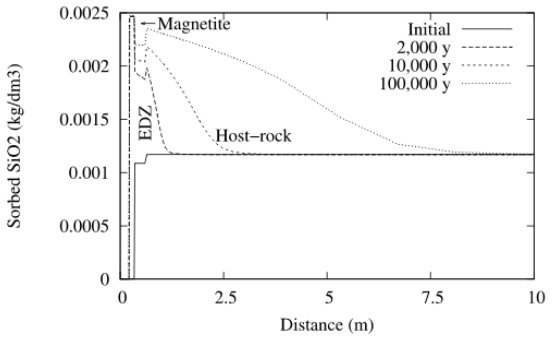

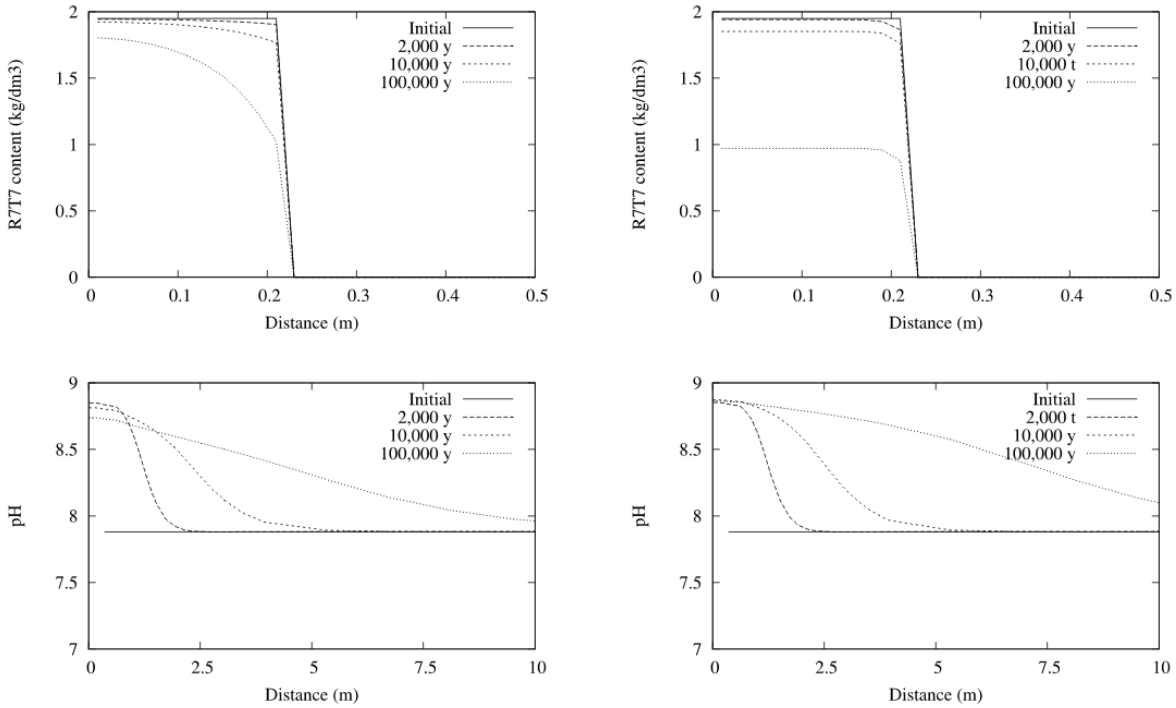

Figure 3. Evolution with time of silica sorption on corroded steel and the host-rock clay minerals, R7T7 contents and pH profiles for test-case III.

increases with time contrarily to the magnetite one. However, the overall process of silica migration and sorption is still diffusion-controlled. Migration is particularly well-restrained due to the low effective diffusion coefficient of the host-rock. The total altered glass fraction only reaches approximately 10% after 100,000 years for the lowest fracturation ratio (see Table II). The dissolution process is more active at the boundary of the vitrified waste zone open to the near-field environment than in the inner zones, likewise test-case I, but in a more accentuated manner (Figure 3). Glass dissolution is essentially driven by the residual rate in the highest fracturation case. As a result, silica sorption has only a slight effect on dissolution as discussed

above. The pH is still buffered by the host-rock minerals, albeit slightly higher compared with test-case I (Figure 3).

These findings are not significantly changed while fitting the surface complexation constant of silica on a Kd value one order of magnitude higher. On the other hand, the results seemed to be more sensitive to the specific surface of clay minerals (20 m^2/g was assumed in the present calculations), i.e. their total number of sorption sites. On the long-term, sorption processes in the

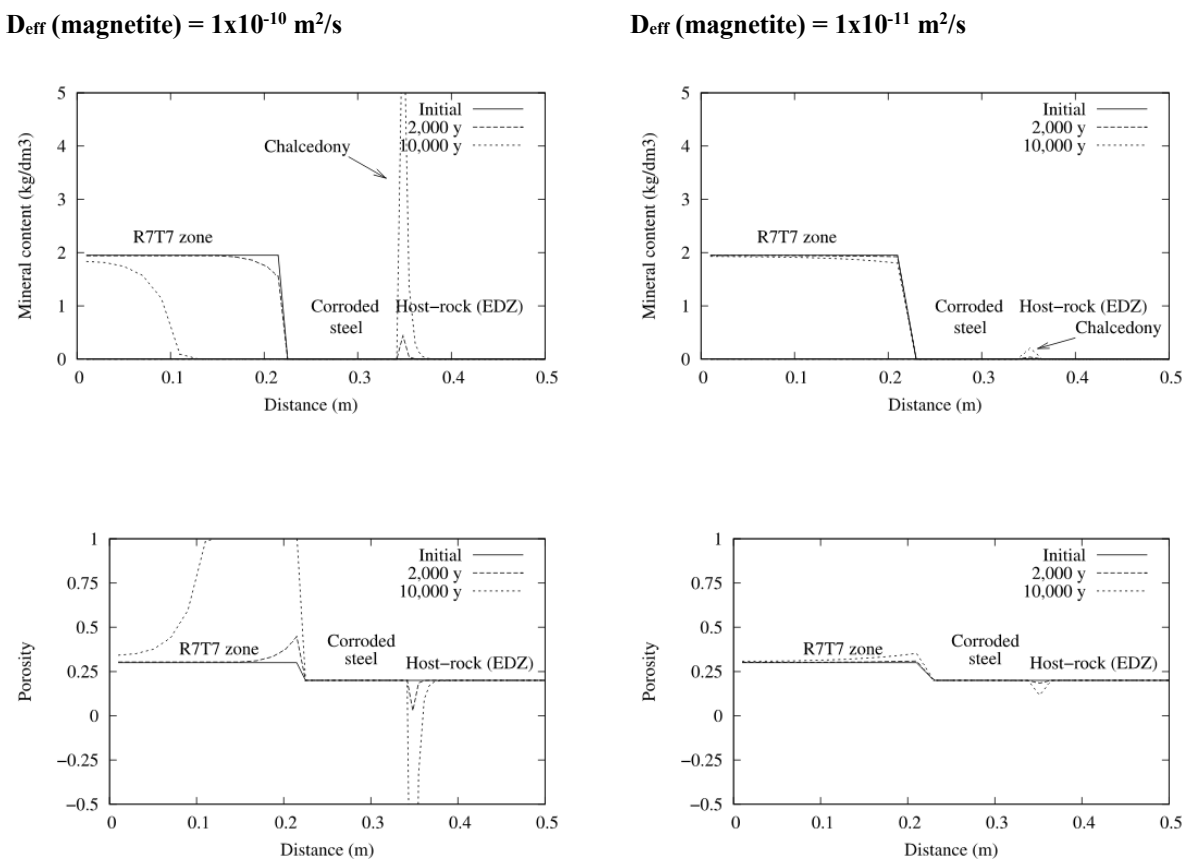

Figure 4. *Top:* progressive alteration of the vitrified waste driven by silicate mineral precipitation in the host-rock (fracturation ratio = 60, test-case IV) with respect to the value assigned to the effective diffusion coefficient of elements in the corrosion products; *bottom*: evolution of the porosity calculated according to the mineral contents but without feedback on diffusion parameters (which can lead to unrealistic negative values for porosity).

host-rock may act as precursors for precipitating silicate minerals such as chalcedony at 50° C [2,4]. As shown in Figure 4, precipitation may affect glass durability much more than sorption in agreement with conclusions drawn in previous modelling studies [5,6]. However, the intensity of glass alteration is dependent on the effective diffusion coefficient $D_{eff\text{-}mag}$ considered for corrosion products. For the lowest $D_{eff\text{-}mag}$, the altered glass fraction remains low. For the highest $D_{eff\text{-}mag}$, the altered glass fraction already approaches 65% after 10,000 years when chalcedony can precipitate. The pH simultaneously increases to a value close to 10, which further catalyses glass dissolution according to Eq 1. At the same time, the precipitation of chalcedony, which is restricted to a narrow zone in the host-rock, leads to a significant drop of porosity (Figure 4). Calculations indicate that a porosity drop reduces diffusive transfer and glass alteration after a few thousand years already. The feedback of mineral precipitation on diffusive transfers was not explicitly taken into account in this first modelling work. At last, Figure 4 also shows that, depending on the assumed effective diffusion coefficient, corrosion products may limit glass dissolution by controlling silica diffusion.

CONCLUSIONS

Sensitivity calculations have been performed according to a modelling study based on a coupled chemistry transport code to assess of the effect of sorption and precipitation processes on R7T7 glass durability. An operational kinetic law was used to describe glass dissolution at realistic time scales and conforming the repository design. The related parametric rate-law

should be updated with respect to new experimental data, since the model is unable to provide by itself for an accurate chemical description of the gel evolution in near-field disposal conditions. This paper focused on silica processes involved in the near-field of the disposal, but other major glass constituents such as aluminium, characterized by a low solubility, should be considered in further calculations. Without silica sorption and precipitation, glass dissolution is diffusion-driven and the fraction of altered glass after 100,000 years ranges from 5% to 50% depending on the fracturation degree of the glass block. Steel corrosion products limit glass dissolution by controlling silica diffusion, whereas silica sorption on magnetite has almost no effect on glass durability. Within the host-rock, precipitation of silicate minerals such as chalcedony may affect glass durability more considerably than sorption. In that case, however, a concomitant porosity drop is predicted that could progressively reduce diffusion and subsequent glass alteration.

ACKNOWLEDGMENTS

This paper benefited from thorough and constructive comments by Drs. M. Aertsens, G. de Combarieu and S. Gin.

REFERENCES

1. E. Vernaz, S. Gin, C. Jégou and I. Ribet, *J. Nucl. Mater.* **298**, 27 (2001).
2. P. van Iseghem, E. Valcke and A. Lodding, *J. Nucl. Mater.* **298**, 86 (2001).
3. P. Jollivet, Y. Minet, M. Nicolas and E. Vernaz, *J. Nucl. Mater.* **281**, 231 (2000).
4. S. Gin, P. Jollivet, J.P. Mestre, M. Jullien and C. Pozo, *Appl. Geoch*. **16**, 861 (2001).
5. M. Aertsens and P. van Iseghem, , ENS Meeting Proc. (Antwerpen, Belgium), 339 (1999).
6. S. Maillard and D. Iracane , Mat. Res. Soc. Symp. Proc. **506**, 231 (1998).

7. J. van der Lee, L. De Windt, V. Lagneau and P. Goblet, *Comp. Geosc.* **29**, 265 (2003).

8. N. Marmier and F. Fromage, *J. Coll. Interf. Sc.* **223**, 83 (2000).

9. V. Philippini, S. Leclercq and H. Catalette, Techn. Rep. EdF HT-29/04/026/A (2004).

10. E. Curti, Techn. Rep. PSI 03-18 (2003).

11. L. De Windt, J. Cabrera and J.-Y. Boisson, *Geol. Soc. London Spec. Publ.* **157**, 167 (1999).

12. M.H. Bradbury and B. Baeyens, *J. Cont. Hydr.* **27**, 223 (1997).

13. B. Grambow and R. Müller, *J. Nucl. Mater.* **298**, 112 (2001).

14. S. Gin and P. Frugier, *Mat. Res. Soc. Symp. Proc.* **757**, 175 (2003).